Journal of Engineering Mathematics, Vol. 13, No. 3, July 1979

The collision of unsteady laminar boundary layers

W. H. H. BANKS and M. B. ZATURSKA

School of Mathematics, University of Bristol, Bristol, U.K.

(Received October 17, 1978 and in revised form December 5, 1978)

SUMMARY

The boundary-layer growth near the equator of an impulsively rotated sphere is considered numerically and analytically. The numerical work is highly suggestive of the presence of a singularity at a finite time at which two of the velocity components and the swirl displacement thickness become infinite. Details of an analytic investigation are presented which is consistent with the gross features of the numerical results. Brief consideration is also given to the flow near the equators of impulsively rotated spheroids and it is shown that the relevant boundary-layer equations for this class of bodies can be written in the same form as those for the sphere.

1. Introduction

There are a number of situations in which two streams of fluid, emanating from two distinct regions, meet and proceed as a single flow. A very simple example concerns the steady flow past a finite flat plate aligned parallel to the oncoming stream: the fluid on one side meets the fluid from the other side (again) at the trailing edge forming the wake. Other and more complicated examples are common: if we consider the steady uniform flow past a sphere for Reynolds number not small the region of separation can be regarded as the junction of two flows, one of which is at some stage in the neighbourhood of the front stagnation point and the other being the reversed flow which passes near the *rear* stagnation point.

An essential feature in each of these examples is the fact that the fluid leaves the rigid body concerned in a fairly abrupt manner. An example without this feature, in which two laminar boundary layers meet and proceed smoothly, occurs at a three-dimensional stagnation point where the geometry is of saddle type. It is found (Davey [1]) that providing c, which is related to the two velocity components of the outer flow, is suitably restricted the confluence and development of the flow proceeds without (a) any discontinuities or (b) the ejection of boundary-layer fluid into the main stream.

However, it is well-known that if the potential flow details are used for a steady boundary layer with an imposed adverse pressure gradient, then there is a singularity at the position at which reversed flow is assumed to first occur and the calculation cannot be continued.

Another approach is to consider the unsteady flow generated by the impulsive motion of a body. The archetypal problem that has been considered in this category is the circular cylinder which is impulsively started in a direction perpendicular to its axis. From the boundary-layer equations the early motion is determined using the method of Blasius [2], but the results are

valid only for small time. Apart from the large-time analysis of Proudman and Johnson [3], at times of $O(1)$ and larger the flow properties are derived numerically by using finite-differences etc. A numerical investigation into the flow development on an impulsively started circular cylinder has been reported by Telionis and Tsahalis [4] in which an 'upwind' finite-difference scheme was used; in this way they were able to integrate the boundary-layer equations for times not small and were able to track the movement of the point on the cylinder which separates forward and backward flow. They found evidence to suggest that a singularity occurred for all $t > t_s$ ($t_s \approx 0.6$ if suitably non-dimensionalised) although it did not occur at the position of zero skin-friction, but was displaced slightly towards the rear stagnation point. No analytic support was presented and the evidence for the singularity was tentative. It is therefore clear that further work on this problem remains to be done to confirm, or otherwise, the existence, and examine the analytical structure, of such a singularity.

However, there are a number of situations, albeit of different type, in which the collision position in an unsteady development is fixed for all time which clearly offers great advantages in any examination of the resulting particular structure. One of these concerns the flow at the equator of a rotating sphere. The sphere of radius a is assumed to rotate with angular velocity Ω about a diameter in otherwise stationary fluid of kinematic viscosity ν, and because of the secondary flow generated, fluid moves in boundary layers (provided $R = a^2\Omega/\nu \gg 1$) over both hemispheres towards the equator where an inevitable collision results. Although the flow properties over most of the sphere, such as the velocity field and drag etc., are believed known, no analytical or numerical details are available in the collision and consequent eruption region.

The advantage of the rotating sphere as a vehicle for the investigation of the unsteady collision process lies in the symmetry of the problem: the collision location is fixed at the equator for all time. The present work is concerned with the flow development at the equator of an impulsively rotated sphere. It should be stressed however that the collision of the boundary layers at the sphere equator clearly cannot be considered as being in any way analogous to the junction of the boundary-layer flow at the position of zero skin-friction on an impulsively started circular cylinder, although where the results of Telionis and Tsahalis and those reported here appear to have features in common we shall merely note the fact without further comment.

The work of Smith and Duck [5] is concerned with the flow near the equator of a rotating sphere, but they consider the steady flow structure which involves effects of order higher than that of first-order boundary-layer theory. The present work, on the other hand, is within the framework of first-order boundary-layer theory.

In Section 2 the problem of the boundary-layer development on an impulsively rotated sphere is posed and the form of the early motion is given. Equations for the local behaviour at the equator are also derived and a series solution for the early flow development is obtained in which the first four non-zero terms are found. Section 3 is concerned with the finite-difference representation and the numerical results are presented in graphical and tabular form in Section 4. A property of the numerical solution is that the normal velocity at the edge of the boundary-layer appears to become singular at a finite time. Section 5 is concerned with an analytical description of the inviscid region in the neighbourhood of the singularity. Graphs are presented which strongly support the structure proposed.

2. Equations of motion

Referred to spherical polar co-ordinates (r, θ, ϕ) where r is the distance from the sphere centre, θ is the polar angle measured from the axis of rotation and ϕ is the azimuthal angle and with the assumption of rotational symmetry the boundary-layer equations are

$$\begin{aligned}
\frac{\partial u}{\partial t} + w\frac{\partial u}{\partial r} + \frac{u}{a}\frac{\partial u}{\partial \theta} - \frac{v^2 \cot\theta}{a} &= \nu \frac{\partial^2 u}{\partial r^2}, \\
\frac{\partial v}{\partial t} + w\frac{\partial v}{\partial r} + \frac{u}{a}\frac{\partial v}{\partial \theta} + \frac{uv\cot\theta}{a} &= \nu \frac{\partial^2 v}{\partial r^2}, \\
\frac{1}{a}\frac{\partial u}{\partial \theta} + \frac{u\cot\theta}{a} + \frac{\partial w}{\partial r} &= 0,
\end{aligned} \tag{1}$$

where w, u and v are the velocity components in the directions of increasing r, θ and ϕ respectively, and a is the radius of the sphere. The initial and boundary conditions are

$$\begin{aligned}
&t < 0: \quad u = v = w = 0, \\
&t > 0: \begin{cases} u = w = 0, \quad v = a\Omega \sin\theta \quad \text{on} \quad r = a, \\ u, v \to 0 \quad \text{as} \quad r \to \infty, \end{cases}
\end{aligned} \tag{2}$$

corresponding to the sphere being given an impulsive angular velocity Ω about the polar axis.

The solution of equations (1) subject to (2) for $T = \Omega t$ small was first considered by Nigam and Rangasami [6] and later by Banks [7]. It can be inferred from these investigations that the solution is of the form

$$\begin{aligned}
u &= a\Omega\mu(1-\mu^2)^{\frac{1}{2}} T\{f_0(\eta) + T^2[f_{21}(\eta) + \mu^2 f_{22}(\eta)] + T^4[f_{41}(\eta) + \mu^2 f_{42}(\eta) + \\
&\quad + \mu^4 f_{43}(\eta)] + \ldots\}, \\
v &= a\Omega(1-\mu^2)^{\frac{1}{2}} \{g_0(\eta) + T^2[g_{21}(\eta) + \mu^2 g_{22}(\eta)] + T^4[g_{41}(\eta) + \mu^2 g_{42}(\eta) + \\
&\quad + \mu^4 g_{43}(\eta)] + \ldots\}, \\
w &= (\nu\Omega)^{\frac{1}{2}} T^{3/2}\{(1-3\mu^2)h_0(\eta) + T^2[(1-3\mu^2)h_{21}(\eta) + \mu^2(3-5\mu^2)h_{22}(\eta)] + \\
&\quad + \ldots\},
\end{aligned} \tag{3}$$

where $\mu = \cos\theta$ and $\eta = \frac{1}{2}(r-a)/(\nu t)^{\frac{1}{2}}$★. The initial functions of η in the above series are determined by the equations

$$\begin{aligned}
&L_0\, g_0 = 0, \quad L_1\, f_0 = -4g_0^2, \quad h_0' - 2f_0 = 0, \\
&L_2(g_{21}, g_{22}) = (2h_0'g_0', \; -6h_0g_0' + 8f_0g_0), \\
&L_3(f_{21}, f_{22}) = (-8g_0g_{21} + 2h_0f_0' - 4f_0^2, \; -8g_0g_{22} - 6h_0f_0' + 8f_0^2), \\
&h_{21}' - f_{21} = 0, \qquad h_{22}' - 2f_{22} = 0,
\end{aligned} \tag{4}$$

★ We note that the form of the solution implies that $u(r, \theta) = -u(r, \pi-\theta)$, $v(r, \theta) = v(r, \pi-\theta)$, $w(r, \theta) = w(r, \pi-\theta)$, and in particular that $u(r, \pi/2) = 0$.

subject to the boundary conditions

$$\begin{aligned} &g_0(0) = 1, \quad g_{21}(0) = g_{22}(0) = 0, \\ &f_0(0) = f_{21}(0) = f_{22}(0) = 0, \\ &g_0(\infty) = g_{21}(\infty) = g_{22}(\infty) = 0, \quad f_0(\infty) = f_{21}(\infty) = f_{22}(\infty) = 0, \\ &h_0(0) = h_{21}(0) = h_{22}(0) = 0, \end{aligned} \tag{5}$$

where

$$L_n \equiv \frac{d^2}{d\eta^2} + 2\eta \frac{d}{d\eta} - 4n.$$

Analytical expressions for the functions g_0, f_0, h_0 were obtained by Nigam and Rangasami while Banks obtained expressions for g_{21} and g_{22} in terms of other known functions. The details are not given here, but the principal properties are

$$\begin{aligned} &g_0'(0) = -2/\sqrt{\pi}, \quad f_0'(0) = 4(1 - 2/\pi)/\sqrt{\pi}, \\ &h_0(\infty) = 4(2/\pi + 1 - \sqrt{2})/(3\sqrt{\pi}), \\ &g_{21}'(0) = -\{35/18 + [-19 + 42\sqrt{3/5}]/\pi - 256/45\pi^2)\}/\sqrt{\pi}, \\ &g_{22}'(0) = \{61/18 - [115/3 - 66\sqrt{3/5}]/\pi + 512/(45\pi^2)\}/\sqrt{\pi}. \end{aligned} \tag{6}$$

No further analytical results are known for the higher-order terms. Although in principle further terms could be found, in practice the amount of algebra increases so rapidly that such an approach becomes prohibitive: even with an automatic computer the wisdom of proceeding in this way must be questionable in view of the unknown degree of convergence. Further work must clearly be by way of finite-differences or their equivalent.

However, the region of interest is at the equator where μ is small and a useful preliminary study would appear to be a local investigation of the flow structure there. Specifically we infer from equations (3) that for small T, the solution is of the form

$$\begin{aligned} u &= a\Omega\mu u'(z, T) + O(\mu^3), \\ v &= a\Omega v'(z, T) + O(\mu^2), \\ w &= (\nu\Omega)^{\frac{1}{2}} w'(z, T) + O(\mu^2), \end{aligned} \tag{7}$$

where

$z = (r - a)(\Omega/\nu)^{\frac{1}{2}}$ and u', v', w' satisfy

$$\begin{aligned} &\frac{\partial u'}{\partial T} + w' \frac{\partial u'}{\partial z} - u'^2 - v'^2 = \frac{\partial^2 u'}{\partial z^2}, \\ &\frac{\partial v'}{\partial T} + w' \frac{\partial v'}{\partial z} = \frac{\partial^2 v'}{\partial z^2}, \\ &u' - \frac{\partial w'}{\partial z} = 0, \end{aligned} \tag{8}$$

with appropriate initial and boundary conditions

$$T = 0: \quad u' = v' = w' = 0,$$
$$T > 0: \begin{cases} u' = w' = 0, & v' = 1 \quad \text{on} \quad z = 0, \\ u', v' \to 0 & \text{as} \quad z \to \infty. \end{cases} \tag{9}$$

Such an investigation whereby a local (or asymptotic) solution is sought is not novel of course, although it must be borne in mind that the interpretation of results so obtained may be questionable for $T \to \infty$, as is usual in any double-limiting procedure. It may be anticipated that the shape of the sphere near the poles will affect the details of the flow pattern at the equator but the assumption here is that the *character* of the flow at the equator is independent of any changes in the body shape in the polar regions.

It is possible to determine the effect of certain equatorial variations in the shape of the body on the flow at the equator by considering the boundary-layer growth at the equators of spheroids. The equations analogous to (8) are derived in the Appendix for rotating spheroids. It will be seen that the influence of equatorial body shape is indeed simply one of degree rather than character; it is shown that the boundary-layer equations for the equator flow due to prolate and oblate spheroids coincides with (8) providing the time variable is transformed suitably. As one might reasonably expect on physical grounds, the time is stretched for prolate spheroids and contracted for oblate spheroids. In short, we may expect that for T not too large the results will be of some value in discussing the general behaviour of the flow near the equator.

The remainder of this investigation is concerned with the solution of (8) subject to (9), and in order to provide a check for the finite-difference investigation presented later, the early motion for these equations was obtained in the form

$$\begin{aligned} u' &= T\{f_0(0) + T^2 f_{21}(\eta) + T^4 f_{41}(\eta) + T^6 f_{61}(\eta) + \dots\}, \\ v' &= g_0(\eta) + T^2 g_{21}(\eta) + T^4 g_{41}(\eta) + T^6 g_{61}(\eta) + \dots, \\ w' &= T^{3/2}\{h_0(\eta) + T^2 h_{21}(\eta) + T^4 h_{41}(\eta) + T^6 h_{61}(\eta) + \dots\}, \end{aligned} \tag{10}$$

where

$$\begin{aligned} f_0(0) &= f_{21}(0) = f_{41}(0) = f_{61}(0) = 0, \\ g_0(0) - 1 &= g_{21}(0) = g_{41}(0) = g_{61}(0) = 0, \\ h_0(0) &= h_{21}(0) = h_{41}(0) = h_{61}(0) = 0, \\ f_0(\infty) &= f_{21}(\infty) = f_{41}(\infty) = f_{61}(\infty) = 0, \\ g_0(\infty) &= g_{21}(\infty) = g_{41}(\infty) = g_{61}(\infty) = 0. \end{aligned}$$

The resulting ordinary differential equations for the function f, g, h were integrated numerically and the properties are given below.

$$f_0'(0) = 0.820061, \quad g_0'(0) = -1.128379, \quad h_0(\infty) = 0.167306,$$
$$f_{21}'(0) = 0.016515, \quad g_{21}'(0) = 0.027468, \quad h_{21}(\infty) = 0.010032,$$
$$f_{41}'(0) = 0.000564, \quad g_{41}'(0) = 0.000405, \quad h_{41}(\infty) = 0.000579,$$
$$f_{61}'(0) = 0.000019, \quad g_{61}'(0) = 0.000004, \quad h_{61}(\infty) = 0.000032.$$

We note that the values for $f_0'(0)$, $g_0'(0)$, $h_0(\infty)$ and $g_{21}'(0)$ given here agree, to the number of figures shown, with the analytical results given in (6). In view of the restricted convergence of such a series solution we proceed to a numerical solution using finite-differences in the next section.

3. Finite-difference formulation

Because of the singularity at $T = 0$ we first write equations (8) in terms of the independent variables η, T where η is defined as before. Hence with

$$u'(z, T) = Tu_1(\eta, T), \quad v'(z, T) = v_1(\eta, T), \quad w'(z, T) = T^{3/2} w_1(\eta, T),$$

the equations for u_1, v_1, w_1 are

$$\begin{aligned} &4u_1 + 4T\frac{\partial u_1}{\partial T} - 2\eta\frac{\partial u_1}{\partial \eta} - 4T^2u_1^2 + 2T^2w_1\frac{\partial u_1}{\partial \eta} - 4v_1^2 = \frac{\partial^2 u_1}{\partial \eta^2}, \\ &4T\frac{\partial v_1}{\partial T} - 2\eta\frac{\partial v_1}{\partial \eta} + 2T^2w_1\frac{\partial v_1}{\partial \eta} = \frac{\partial^2 v_1}{\partial \eta^2}, \\ &\frac{\partial w_1}{\partial \eta} - 2u_1 = 0. \end{aligned} \tag{11}$$

The method followed in this investigation was to use these equations from $T = 0$ to some convenient value of T, say T_0, and to proceed from $T = T_0$ using a modified form of the equations (8). The modification consists of using a stretched variable normal to the boundary by writing $\zeta = \log(1 + z/2\,T_0^{\frac{1}{2}})$, so that in terms of this variable equations (8) become

$$\begin{aligned} &\frac{\partial u'}{\partial T} + \frac{e^{-\zeta}w'}{2T_0^{\frac{1}{2}}}\frac{\partial u'}{\partial \zeta} - u'^2 - v'^2 = \frac{e^{-2\zeta}}{4T_0}\left[\frac{\partial^2 u'}{\partial \zeta^2} - \frac{\partial u'}{\partial \zeta}\right], \\ &\frac{\partial v'}{\partial T} + \frac{e^{-\zeta}w'}{2T_0^{\frac{1}{2}}}\frac{\partial v'}{\partial \zeta} = \frac{e^{-2\zeta}}{4T_0}\left[\frac{\partial^2 v'}{\partial \zeta^2} - \frac{\partial v'}{\partial \zeta}\right], \\ &\frac{e^{-\zeta}}{2T_0^{\frac{1}{2}}}\frac{\partial w'}{\partial \zeta} - u' = 0. \end{aligned} \tag{12}$$

The motivation for this non-uniform stretching comes from noting that typical boundary-layer profiles have exponential-type decay away from the boundary and the transformation used was chosen to accomodate the decay region without the introduction of a large number of grid points. It has been used previously (Banks [8]) for boundary-layer calculations and was found very useful. We note that as a consequence of this stretching, interpolation was necessary at $T = T_0$ in order to obtain values of the dependent variables at the grid points in the (ζ, T)-plane. However this process was checked by using different orders for the interpolating polynomial and confirming that any discrepancies were small. Comparison with the small T analysis of Section 2 is made later, but this interpolation procedure was also checked by comparing the results obtained by integrating (11) to some time $T_1 (> T_0)$ with the results derived by integrating equations (12), via the interpolated values at T_0.

The sets of equations in both (11) and (12) were integrated using the Crank-Nicolson method. This was used in a previous study (see Banks [8]) where full details are given. Briefly, the method assumes a grid in the η, T (or ζ, T)-plane and the various derivatives are replaced by their finite-difference approximations centred on a typical point $\{(i+\frac{1}{2})k, jh\}$, where h, k denote the step-lengths in the η, T directions respectively; a typical quantity $f\{(i+\frac{1}{2})k, jh\}$ is then written as an average of $f(ik, jh)$ and $f\{(i+1)k, jh\}$. The continuity equation is integrated using the trapezoidal rule. The boundary conditions at inifinity are imposed at $\eta = Nh$ where N is chosen large enough so that not only does the appropriate function equal its boundary value but also the derivative is very small. The problem at each time step is thus reduced to the solution of 2N-2 non-linear algebraic equations for the unknowns $u_{i+1,j}, v_{i+1,j} (1 \leqslant j \leqslant N\text{-}1)$ in terms of the known $u_{i,j}$ and $v_{i,j}$; Newton's iterative method using Gaussian elimination was employed for this purpose.

The procedure followed was to continue with the iteration until the magnitude of the difference of two successive iterates be less than a specified tolerance, $\epsilon^{\star}$, at which stage convergence is assumed and the time is advanced by one grid spacing. The value chosen for ϵ in all the present calculations was 10^{-6}. It may be anticipated that $N = N(T)$ and we have adjusted N at each stage of the calculation to ensure that at the position where the boundary conditions were imposed the appropriate derivatives were also small. It was found, for example, that over the time interval (2,4.5) z varied from about 20 to 66 but it was only necessary to increase N by about 40%.

4. Numerical results

Preliminary numerical experiments were performed to get some impression of the overall character. From these results it was possible to assess the position at which the outer boundary condition could be imposed and also the size of the time steps. It transpired that the finite-difference solution was not very sensitive to changes in the time step-length compared with changes in the space step-length, although we have nevertheless used the Richardson extrapolation procedure in both. This procedure was checked by using results from at least three different values

* In cases like that presented here, it is possible that a more useful criterion away from the zeros is to consider the relative difference when comparing successive iterates.

TABLE 1

The finite-difference results (F.D.) compared with four terms of the series solution in Section 2.

T	$\left(\frac{\partial u'}{\partial z}\right)_0$		$\left(\frac{\partial v'}{\partial z}\right)_0$		$w'(\infty,T)$	
	Series	F.D.	Series	F.D.	Series	F.D.
0.25	0.20527	0.20527	−1.12666	−1.12668	0.02099	0.02099
1.0	0.41858	0.41855	−0.55025	−0.55029	0.17795	0.17791
1.5	0.52682	0.52681	−0.43455	−0.43460	0.35488	0.35490
2.0	0.63382	0.63395	−0.35771	−0.35773	0.61871	0.62016
3.0	0.89047	0.89619	−0.24399	−0.24418		

of the step-lengths. Further, the skin-friction components $(\partial u'/\partial z)_0$, $(\partial v'/\partial z)_0$ and the normal velocity at the edge of the boundary layer, $w'(\infty,T)$, were compared with the values from the series expansion of Section 2 and the agreement was satisfactory for T not too large. Table 1 gives more details and it will be seen that the series solution for $(\partial u'/\partial z)_0$ and $(\partial v'/\partial z)_0$ is convergent for $T \doteq 2$ although that for $w'(\infty, T)$ is not quite so good.

The iterations in the numerical integration converged satisfactorily at each time step for $T \leqslant 4.57$ (the extent to which the integration was carried out) but the corrections, calculated using the Richardson extrapolation procedure, were increasing in magnitude as T increased. We have given here only the results for $T \leqslant 4.56$, beyond which the accuracy becomes doubtful.

A number of facts were evident from the preliminary programme tests. It was noted that the maximum value of the u'-velocity component was increasing as was the w'-velocity at the edge

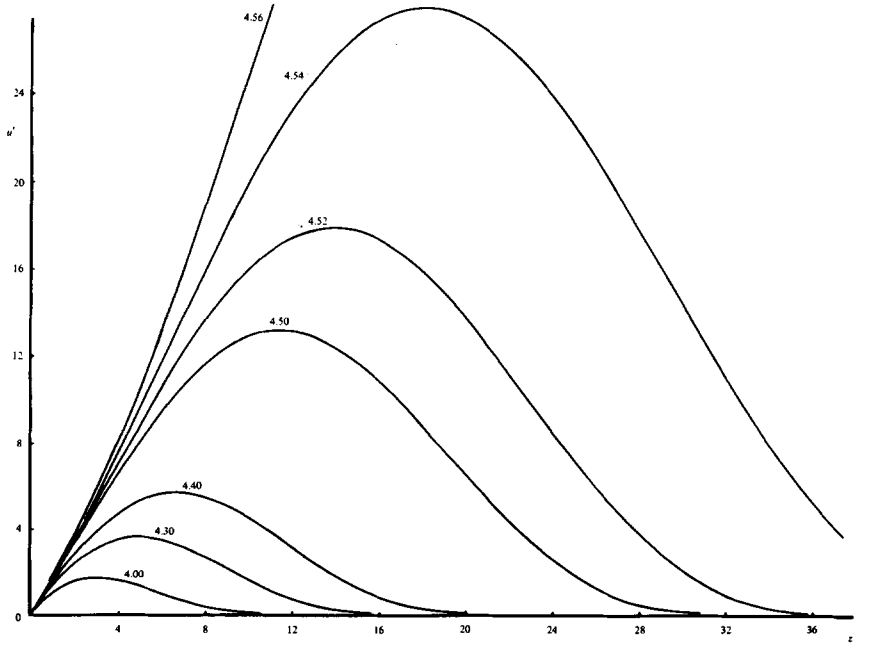

Figure 1. Meridional velocity u' *vs.* z for various times as indicated.

of the boundary layer. In view of this the computer programme was modified to calculate the maximum value of u, say u_m, and also its location, say z_m. Figures 1, 2 and 3 show the variation of u', v', and w' respectively for various times, while Figure 4 gives the variation of $[u'(z_m, T)]^{-1} = (u_m')^{-1}$ say, and $[w'(\infty, T)]^{-2/3} = (w_\infty')^{-2/3}$ say. For $T > 4$ the variation in the latter two quantities in each case is almost linear and we give the relevant numerical results in Table 2. In view of the variation of $u'(z_m, T)$ and $w'(\infty, T)$ we show the variation of z_m^{-2} with

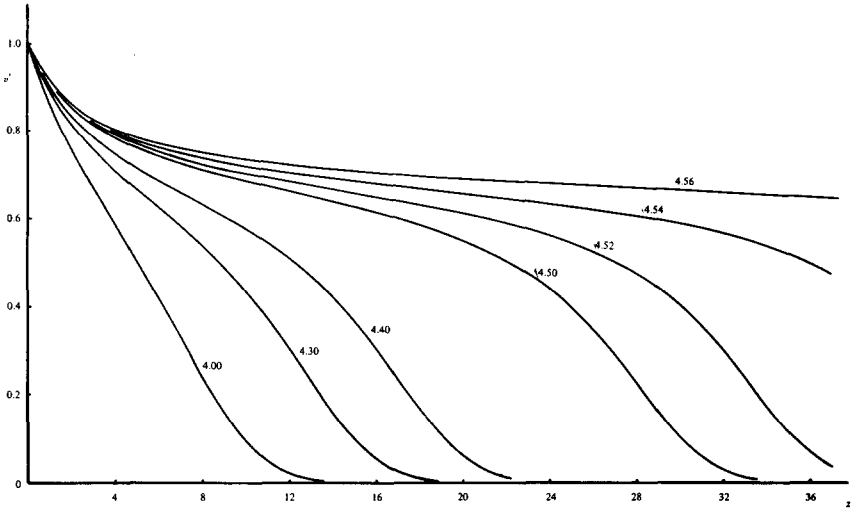

Figure 2. Azimuthal velocity v' *vs.* z for various times as indicated.

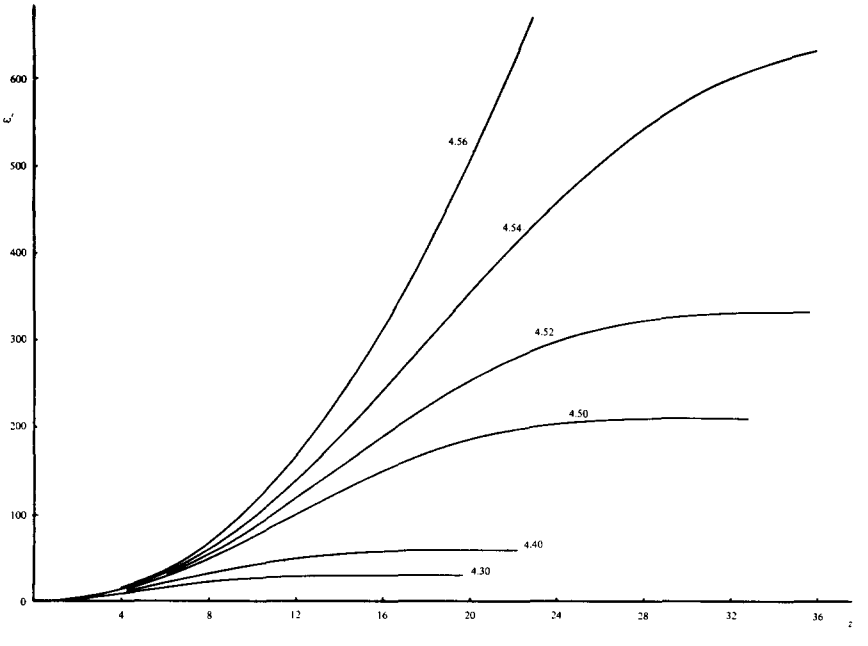

Figure 3. Radial velocity w' *vs.* z for various times as indicated.

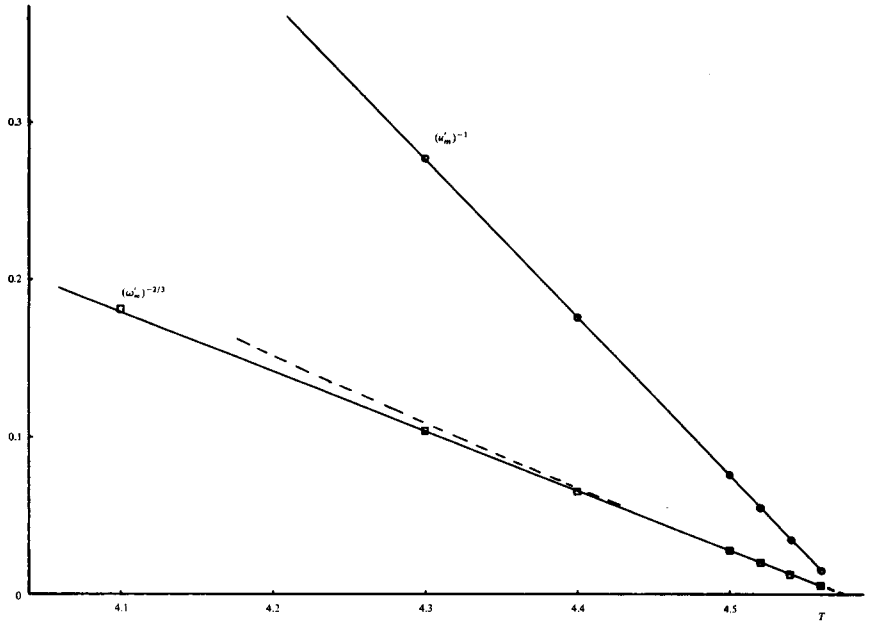

Figure 4. The variation of $(u'_m)^{-1}$ and $(w'_\infty)^{-\frac{2}{3}}$ is shown by circles and squares respectively. Straight (continuous) lines have been drawn for comparison in each case. The value of $(w'_\infty)^{-\frac{2}{3}}$ from the asymptotic results of Section 5 are shown by a broken line.

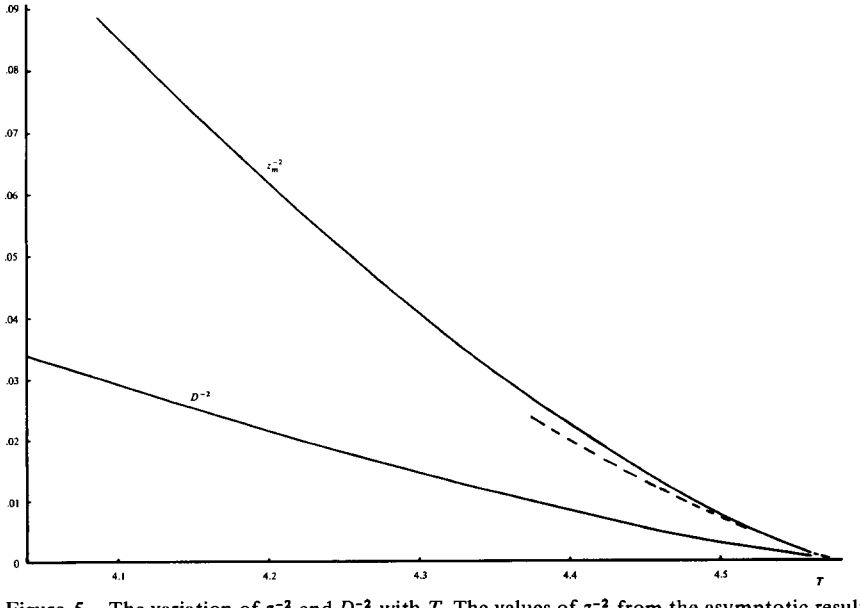

Figure 5. The variation of z_m^{-2} and D^{-2} with T. The values of z_m^{-2} from the asymptotic results of Section 5 are shown by a broken line.

T in Figure 5. At each time step we have also calculated the dimensionless displacement thickness associated with the azimuthal velocity component. We write $D = \int_0^\infty v'dz$ and evaluate the integral using the trapezoidal rule. It transpires that D is another increasing function of T, and we have plotted D^{-2} as a function of T also in Figure 5. Figure 6 gives the variation of the skin-friction components $(\partial u'/\partial z)_0$, $(\partial v'/\partial z)_0$ and the latter is also tabulated in Table 2 to show the linearity for $T > 4$; we note that both components appear to be bounded and non-zero for $T > 0$, and with no exceptional behaviour.

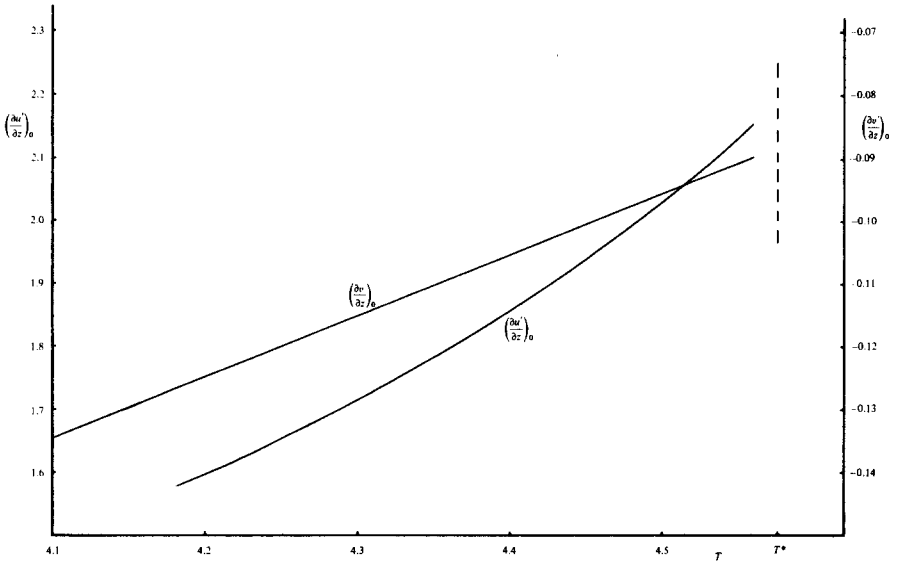

Figure 6. The variation of the skin-friction components $\left(\frac{\partial u'}{\partial z}\right)_0$ and $\left(\frac{\partial v'}{\partial z}\right)_0$ with T.

TABLE 2

T	$[u'(z_m, T)]^{-1}$	$[w'(\infty, T)]^{-2/3}$	$\left(\frac{\partial v'}{\partial z}\right)_0$
4.00	0.58768	0.22109	−0.1446
4.10	0.48256	0.18148	−0.1347
4.20	0.37916	0.14247	−0.1248
4.30	0.27714	0.10398	−0.1150
4.34	0.23662	0.08871	−0.1111
4.38	0.19626	0.07351	−0.1072
4.42	0.15603	0.05838	−0.1033
4.44	0.13595	0.05084	−0.1013
4.46	0.11588	0.04331	−0.0994
4.48	0.09585	0.03580	−0.0975
4.50	0.07581	0.02830	−0.0955
4.52	0.05580	0.02082	−0.0936
4.54	0.03581	0.01335	−0.0917
4.56	0.01579	0.00588	−0.0897

From the results presented here it seems reasonable to conclude that a singularity develops at a finite time T^*. Linear interpolation based on the values of $[u'(z_m, T)]^{-1}$ and $[w'(\infty, T)]^{-2/3}$ at $T = 4.52$ and $T = 4.54$ gives the same value of T^*, viz. $T^* = 4.5758$. We do not claim that this value is accurate for the boundary-layer problem posed in Section 2, but rather that it is fairly accurate for the results presented here, and in any comparison with analytical work only the latter is relevant. It is of interest to note that these results suggest a breakdown before the sphere has completed one revolution, and we may consequently anticipate that these results are applicable to the flow in the vicinity of the equator. It may also be opportune to note that the breakdown found by Telionis and Tsahalis for the impulsively started circular cylinder occurred before the cylinder had moved a distance equal to its diameter.

Attention is drawn to the variation of z_m^{-2} and D^{-2} with T in Figure 5; these results are highly suggestive of both z_m and D becoming singular and are consistent with a scaling $z \sim (T^* - T)^{-\frac{1}{2}}$ as $T \to T^*$. However we find that z_m and D are more accurately represented in the interval $T = 4.10$ to $T = 4.56$ by the functions $(T^* - T)^{-2/3}$ and $(T^* - T)^{-3/5}$ respectively. The former is inconsistent with other results and so is rejected as a possible scaling. In Section 5, where we consider an analytic description, we adopt the simplest hypothesis viz. $z \sim (T^* - T)^{-\frac{1}{2}}$.

Figure 2 suggests that v' remains bounded for all $T < T^*$, and indeed it can be shown that the v'-velocity profile must be monotonic in z so that a maximum in v' cannot form in the interval $0 < z < \infty$. For if at some time a local maximum did form then we can infer by continuity that at an earlier time there would exist a value of z, say z_1, at which

$$\left(\frac{\partial v'}{\partial z}\right)_{z_1} = \left(\frac{\partial^2 v'}{\partial z^2}\right)_{z_1} = 0$$

and with $(\partial^3 v'/\partial z^3)_{z_1} < 0$. However, the momentum equation for v' then implies that

$$\frac{\partial}{\partial T}\left(\frac{\partial v'}{\partial z}\right)_{z_1} < 0$$

and so we conclude that a profile with a local maximum cannot develop. This latter property is not necessarily a property of the finite-difference equations, and the computer programme was modified to include a test for such a possibility. When non-monotonic behaviour occurred in the v'-profile the integration was terminated and the occurrence was taken to imply that the step lengths were too large.

After the numerical results presented above had been obtained we learned that Bodonyi and Stewartson [9] had encountered similar behaviour in the study of an unsteady laminar boundary layer on a rotating disc in a counter-rotating fluid. They were able to proceed to a partial analytical description which seemed to describe the major part of the flow field. We proceed likewise here.

5. Analytical description

In view of the properties presented above we investigate the possibility of an asymptotic solution in which

$$w' = \tau^{-3/2} H(Z, \tau), \quad v' = G(Z, \tau) \tag{13}$$

where $\tau = T^* - T$ and $Z = z\tau^{\frac{1}{2}}$. The equations for the functions $H(Z, \tau)$ and $G(Z, \tau)$ are

$$\begin{aligned} H_Z - \tau H_{Z\tau} - \tfrac{1}{2} Z H_{ZZ} + H H_{ZZ} - H_Z^2 - \tau^2 G^2 &= \tau^2 H_{ZZZ}, \\ \tau G_\tau - \tfrac{1}{2} Z G_Z + H G_Z &= \tau^2 G_{ZZ}, \end{aligned} \tag{14}$$

and the boundary conditions (9) imply that

$$\begin{aligned} &H(0, \tau) = H_Z(0, \tau) = 0, \quad G(0, \tau) = 1, \\ &H_Z(Z, \tau) \to 0, \quad G(Z, \tau) \to 0 \quad \text{as} \quad Z \to \infty. \end{aligned}$$

The initial condition is replaced by the requirement that H and G join on to the numerical results of Section 4 for $\tau \ll 1$.

Note however that since $0 \leqslant v' \leqslant 1$ we may anticipate, and the first of equations (14) confirms, that the role of $G(Z, \tau)$ in the determination of $H(Z, \tau)$ will be weak for $\tau \ll 1$ over most of the flow field. We have re-plotted the u', w', v' velocity profiles in the form $\tau u'(Z, \tau)$, $\tau^{3/2} w'(Z, \tau)$ and $v'(Z, \tau)$ for various values of T; these are given in Figures 7, 8 and 9 respectively and are

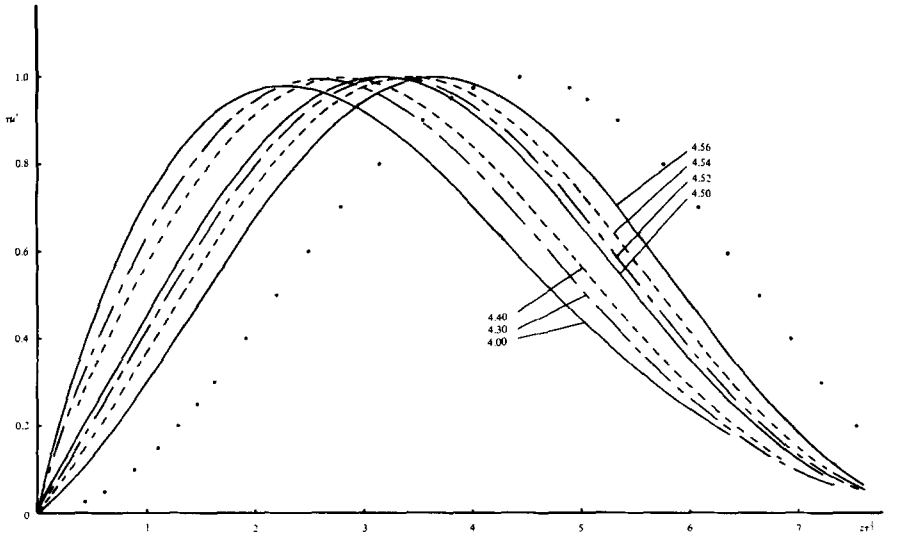

Figure 7. The variation of $\tau u'$ with $Z = z\tau^{\frac{1}{2}}$ for various times as indicated. The dots represent $H_0' = \frac{1}{2}(1-\cos\beta Z)$ (see equation (16)) with $\beta = 0.71$.

suggestive of the probable existence of a simple similar solution valid over most of the flow field. We therefore proceed to look for a solution of the form of (13) with

$$H(Z, \tau) = H_0(Z) + \tau^p H_1(Z) + \ldots,$$
$$G(Z, \tau) = G_0(Z) + \tau^q G_1(Z) + \ldots, \tag{15}$$

where p and q will be chosen later. Because of the passive role played by G in the determination of H we consider first the equation for H.

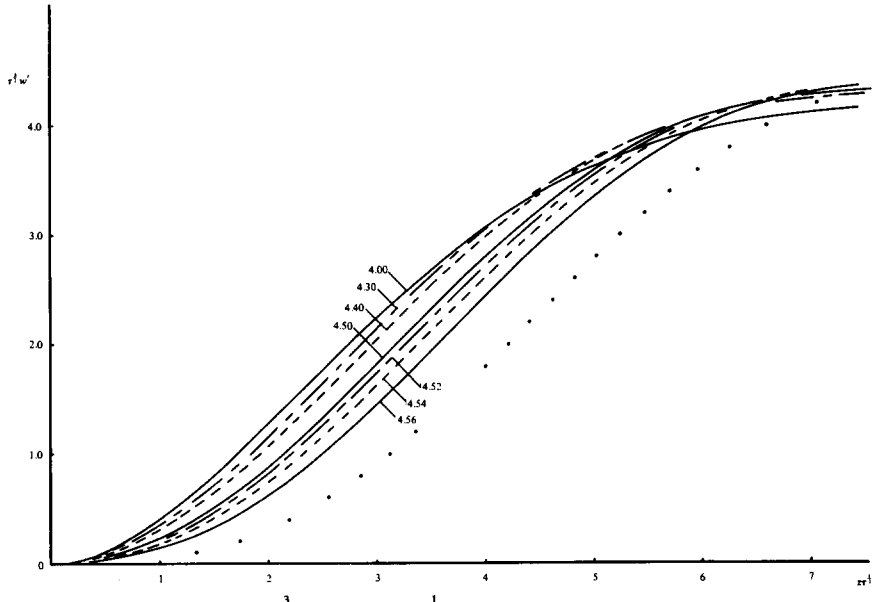

Figure 8. The variation of $\tau^{\frac{3}{2}}w'$ with $Z = z\tau^{\frac{1}{2}}$ for various times as indicated. The results of calculations using equation (16) with $\beta = 0.71$ are shown by dots.

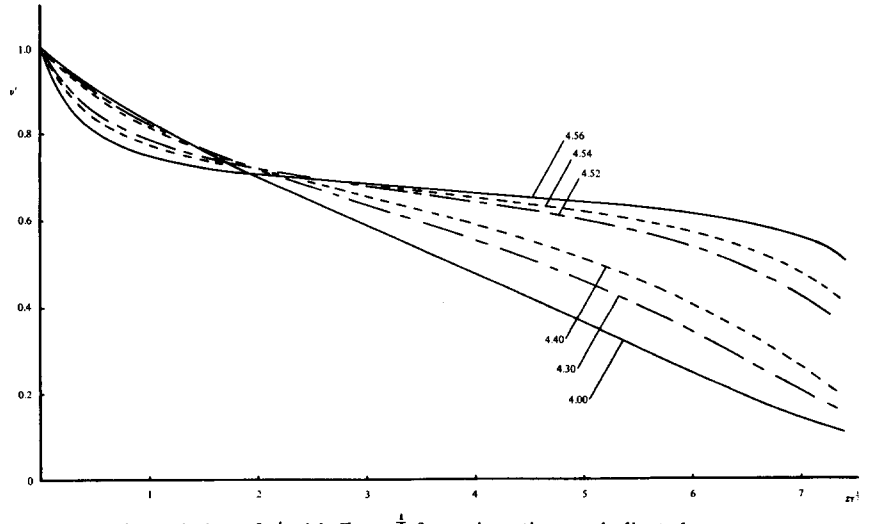

Figure 9. The variation of v' with $Z = z\tau^{\frac{1}{2}}$ for various times as indicated.

Substituting (15) into the first equation of (14) and equating coefficients of τ^0 we obtain

$$(H_0 - \tfrac{1}{2}Z)H_0'' - H_0'^2 + H_0' = 0.$$

The general solution is

$$H_0 = \tfrac{1}{2}Z + A_0 \sin(\beta Z + \gamma),$$

where A_0, β, γ are constants and we have assumed $\beta^2 > 0$ in order to reject exponential forms. One boundary condition is that $H_0(0) = 0$ and, in order that u' be bounded near $z = 0$ as $\tau \to 0$, we also require $H_0'(0) = 0$. These boundary conditions imply that $\gamma = 0, A_0 = -\frac{1}{2}\beta$. Hence

$$H_0 = \tfrac{1}{2}Z - \tfrac{1}{2}\beta^{-1} \sin\beta Z, \tag{16}$$

where β is an undetermined constant the occurrence of which is common in such asymptotic expansions: the usual practice is to choose β suitably so that the form of H_0 'fits' the numerical results as $T \to T^*$ as closely as possible. It is clear that since (16) is an inviscid solution it is not uniformly valid: conditions at $z = 0$ and as $z \to \infty$ are not satisfied; in particular the first of the equations in (8) implies that $\partial^2 u/\partial z^2 = -1$ at $z = 0$ but this cannot be satisfied by (16). We therefore envisage viscous regions bounding the inviscid region. This is similar to the behaviour found by Bodonyi and Stewartson [9]. Ockendon [10] has discussed the steady flow due to a rotating disc with suction and found that there was an inviscid region bounded by thin viscous layers. The boundary condition as $z \to \infty$ is that $u' \to 0$ and so in the relevant viscous region we require the appropriate flow property to match on to (16) and also satisfy $u' \to 0$ at the outer edge. For this to be possible we require u' to be bounded as $\tau \to 0$ in this region and Figures 7 and 8 suggest that the match with (16) must be made at $\beta Z = 2\pi$.

The next stage in applying the method of matched asymptotic expansions is to consider those regions where the above first term fails to be a good approximation. Unfortunately we do not know the structure of the solution in these regions and so we are unable to proceed in a conventional manner. However it is possible to test the form of (16) by comparing with the numerical results after suitably choosing β. Because of the similarity of the H_Z – profiles for $0.2 < H_Z \leqslant 1$, as demonstrated in Figure 7, we choose β by requiring that the *difference* in the two values of Z at which $H_Z = \frac{1}{2}$ be the same in H_0' and in the numerical results. On carrying out the details we find $\beta \approx 0.71$ and for purposes of comparison have plotted H_0 and H_0', with this value of β, in Figures 8 and 7 respectively. The general agreement between the numerical results of Section 4 and the analytical result (16) is sufficiently encouraging for us to proceed with this expansion, although the practice of developing a single non-uniformly valid asymptotic expansion is not without its attendant dangers of course.

If we ignore the effects of the two viscous regions at $Z = 0$ and $Z = 2\pi/\beta$ and proceed to higher-order terms in the inviscid solution, we find that on equating terms of $O(\tau^p)$ the equation for $H_1(Z)$ is

$$(H_0 - \tfrac{1}{2}Z)H_1'' + (1 - p - 2H_0')H_1' + H_0'' H_1 = 0$$

providing $p < 2$. The latter is consistent with the numerical results. One complementary function is $(2p - \cos\beta Z)$ and to ensure that no fractional powers of Z arise in the behavior for small Z, the smallest value of p is $p = \frac{1}{2}$. The general solution is then

$$H_1 = A_1(1 - \cos\beta Z) + B_1\{(1 - \cos\beta Z)\log(1 - \cos\beta Z) + 2\}$$

and $H_1(0) = 0$ implies $B_1 = 0$. Hence

$$H_1 = A_1(1 - \cos\beta Z) \tag{17}$$

which we note satisfies $H_1'(0) = 0$ and $H_1'(2\pi/\beta) = 0$. A_1 is a second undetermined constant. The next term in the expansion of $H(Z, \tau)$ we take to be $\tau H_2(Z)$ and the equation for the determination of $H_2(Z)$ is

$$(H_0 - \tfrac{1}{2}Z)H_2'' - 2H_0' H_2' + H_0'' H_2 = H_1'^2 - H_1 H_1'',$$

the general solution of which is

$$H_2 = \beta A_1^2 \sin\beta Z + A_2(2 - \cos\beta Z) + B_2\{\beta Z(2 - \cos\beta Z) + 3\sin\beta Z\}.$$

The conditions $H_2(0) = H_2'(0) = 0$* are satisfied provided $A_2 = 0, B_2 = -\beta A_1^2/4$, and so

$$H_2 = \tfrac{1}{4}\beta A_1^2\{\sin\beta Z - \beta Z(2 - \cos\beta Z)\}. \tag{18}$$

We note that $H_2'(2\pi/\beta) = 0$.

We have proceeded to the next term which we have taken to be $\tau^{3/2} H_3(Z)$: the equation for H_3 is

$$(H_0 - \tfrac{1}{2}Z)H_3'' - (\tfrac{1}{2} + 2H_0')H_3' + H_0'' H_3 = 2H_1' H_2' - H_1 H_2'' - H_2 H_1'',$$

the general solution of which is

$$H_3 = -\frac{\beta^2 A_1^3}{6}(4\cos\beta Z + 3\beta Z\sin\beta Z) + A_3(3 - \cos\beta Z) + B_3 f(Z),$$

where

$$f(Z) = (3 - \cos\beta Z)\log(1 - \cos\beta Z) + 8.$$

We impose $B_3 = 0$ to avoid a singularity at $\cos\beta Z = 1$, and satisfying $H_3(0) = 0$ implies that $A_3 = \beta^2 A_1^3/3$. Hence

$$H_3 = \beta^2 A_1^3(1 - \cos\beta Z - \tfrac{1}{2}\beta Z\sin\beta Z), \tag{19}$$

which we note satisfies $H_3'(0) = 0$ but that $H_3'(2\pi/\beta) \neq 0$.

* B_2 appears to be another undetermined constant. The numerical results suggest that B_2 is evaluated by satisfying $H_2'(0) = 0$.

The formal expansion of $H(Z, \tau)$ up to the stage considered here is independent of the azimuthal velocity component, although if the next term is taken to be $\tau^2 H_4(Z)$ then viscous and three-dimensional effects enter into the determination of $H_4(Z)$. However, we content ourselves here with the expansion up to and including the term of $O(\tau^{3/2})$ as derived above and note that there are two undetermined constants β and A_1 arising. We summarise these results by giving the expansion of w':

$$w' = \beta^{-1}\tau^{-3/2}\left[\tfrac{1}{2}(\beta Z - \sin\beta Z) + \beta A_1(1-\cos\beta Z)\tau^{\frac{1}{2}} + \tfrac{1}{4}\beta^2 A_1^2\{\sin\beta Z - \beta Z(2-\cos\beta Z)\}\tau \right.$$
$$\left. + \beta^3 A_1^3(1-\cos\beta Z - \tfrac{1}{2}\beta Z\sin\beta Z)\tau^{3/2} + \ldots\right]. \qquad (20)$$

We have tabulated $H(Z, \tau)$ and $H_Z(Z, \tau)$ using the four terms, for various values of β and A_1, and found that with $\beta = 0.71$ and $A_1 = 3.2$ the analytical results join onto the numerical results in a satisfactory manner. For comparison, we have plotted $H(Z, \tau)$ and $H_Z(Z, \tau)$ in Figures 11 and 10 respectively for $T = 4.56$ ($\tau = 0.0158$) and the similarity in each case is most convincing. The agreement for larger values of τ is qualitatively good, although as might be expected the quantitative agreement gets progressively worse as τ increases. From these asymptotic results we find that

$$(u'_m)^{-1} = \tau + O(\tau^{5/2}), \quad (w'_\infty)^{-2/3} = (\beta/\pi)^{2/3}(\tau + \beta^2 A_1^2\,\tau^2/3 + \ldots)$$

and

$$z_m^{-2} = (\beta/\pi)^2(\tau + 4\beta A_1\,\tau^{3/2}/\pi + \ldots).$$

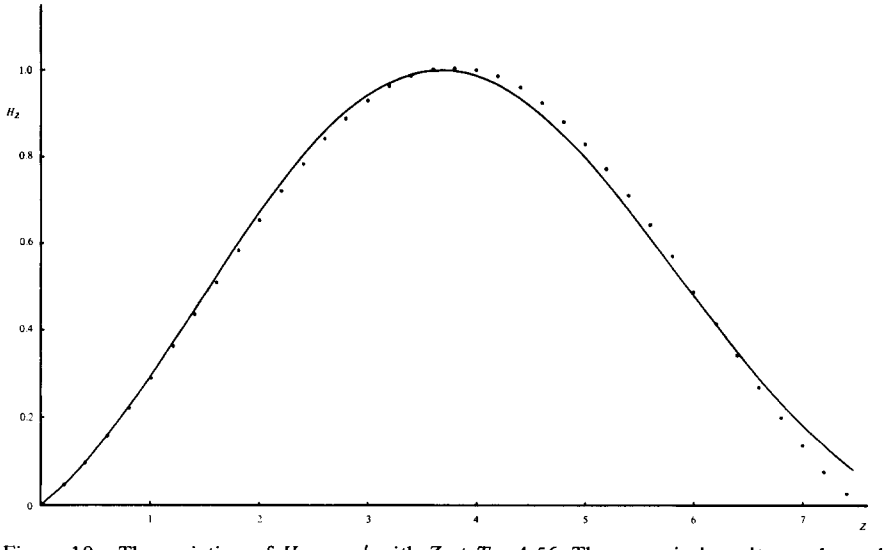

Figure 10. The variation of $H_Z = \tau u'$ with Z at $T = 4.56$. The numerical results are shown by a continuous line and the results from the asymptotic analysis of Section 5 are indicated by dots.

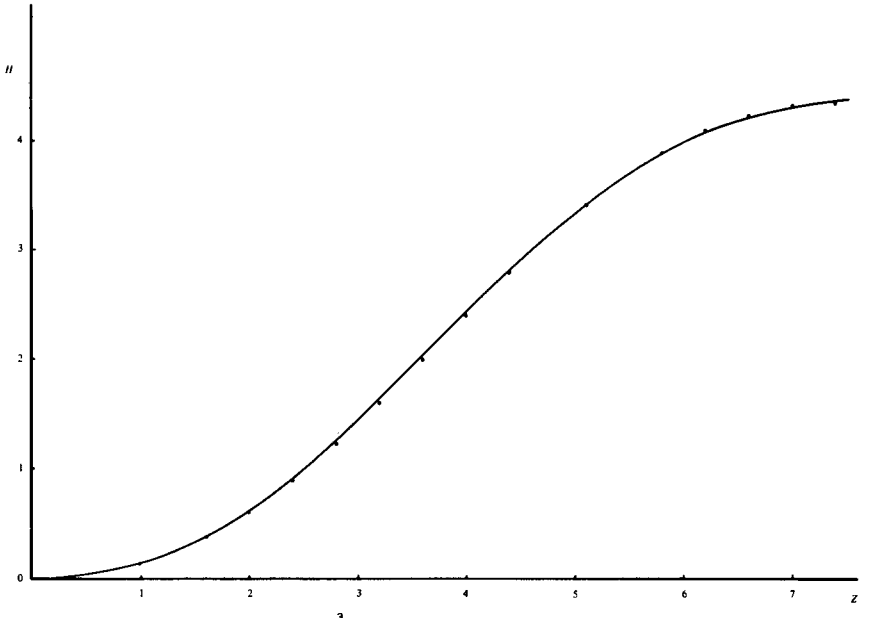

Figure 11. The variation of $H = \tau^{\frac{3}{2}} w'$ with Z at $T = 4.56$. The numerical results are shown by a continuous line and the results from the asymptotic analysis of Section 5 are indicated by dots.

The almost linear variation of $(u'_m)^{-1}$ with τ is consistent with the numerical results which are shown in Figure 4 and Table 2. The variation of $(w'_\infty)^{-2/3}$ and z_m^{-2} with τ given by the analytic results is shown in Figures 4 and 5 respectively, and the agreement is again good for τ small.

Proceeding to the second equation in (14) we find that substitution of the expansions in (15) gives rise to

$$(H_0 - \tfrac{1}{2}Z)G'_0 = 0$$

on equating coefficients of τ^0. The solution of this equation is $G_0 = a_0$, a constant. A reference to Figure 9 suggests that to $o(1)$ this is consistent and that $a_0 \approx 0.7$, although the approximation clearly fails near $z = 0$ and as $z \to \infty$. Whether a_0 is another undetermined constant or is evaluated at a later stage in the matching is not known.

If we proceed with this inviscid expansion and equate coefficients of τ^q we obtain

$$(H_0 - \tfrac{1}{2}Z)G'_1 - q\,G_1 = 0,$$

the general solution of which is $G_1 = a_1 \{\cot(\beta Z/2)\}^{2q}$ where a_1 is a constant. This form of G_1 is clearly singular at $Z = 0$ and $Z = 2\pi/\beta$ for all $q > 0$, and further progress with this expansion is unlikely to be of any value. There are a number of possible explanations for this breakdown but we have been unable to resolve the difficulty.

However, the agreement between the numerical and analytical results for w' and u' as displayed in Figures 10 and 11 is so good that we can infer that the existence of the singularity is confirmed, and that its structure is partly given by the expansion presented here.

6. Discussion

Although the unsteady problem discussed here appears to be substantially different from that of the boundary-layer development on an impulsively started circular cylinder, nevertheless both do involve the interaction of two opposing boundary layers. In the above the position of this juncture of the two equal but oppositely moving boundary layers is fixed for all time, whereas the separating streamline in the cylinder problem moves forward in the direction towards the front stagnation point. Further, the separating streamline is presumably not, even locally, a line of symmetry of the flow pattern. However, it is of interest to note that our results imply that the velocities near to the equatorial plane are of the form $u \sim a\Omega\cos\theta(T^*-T)^{-1}$ and $w \sim (\nu\Omega)^{\frac{1}{2}}(T^*-T)^{-3/2}$ as $T \to T^*$, and in a numerical integration of (1) subject to (2) the term of most significance near the equator will clearly be w; this is also the dominant effect reported by Telionis & Tsahalis [4].

Appendix

We here discuss the boundary-layer development at the equator of an oblate spheroid rotating about its axis. Conventional oblate spheroidal coordinates ξ, η, ϕ are first introduced with $\mathbf{r}(\xi,\eta,\phi) = (c\cosh\xi\sin\eta\cos\phi, c\cosh\xi\sin\eta\sin\phi, c\sinh\xi\cos\eta)$ $(0 \leqslant \eta \leqslant \phi, 0 \leqslant \phi \leqslant 2\pi)$. The boundary-layer equations for the flow are then expressed in terms of coordinates η, ϕ, x_3 where the position vector $\mathbf{R}(\eta, \phi, x_3) = \mathbf{r}(\xi_0, \eta, \phi) + x_3\,\mathbf{n}$ and $\mathbf{n}$ is the outwardly directed unit vector normal to the oblate spheroidal surface defined by $\xi = \xi_0$. Then, with u, v, w representing velocity components in directions corresponding to η, ϕ, x_3 increasing, and with the further assumption of rotational symmetry of the flow, the boundary-layer equations are:

$$\frac{\partial u}{\partial t} + \frac{u}{c(\sinh^2\xi_0 + \cos^2\eta)^{\frac{1}{2}}}\frac{\partial u}{\partial \eta} + w\frac{\partial u}{\partial x_3} - \frac{v^2\cot\eta}{c(\sinh^2\xi_0 + \cos^2\eta)^{\frac{1}{2}}} = \nu\frac{\partial^2 u}{\partial x_3^2},$$

$$\frac{\partial v}{\partial t} + \frac{u}{c(\sinh^2\xi_0 + \cos^2\eta)^{\frac{1}{2}}}\frac{\partial v}{\partial \eta} + w\frac{\partial v}{\partial x_3} + \frac{uv\cot\eta}{c(\sinh^2\xi_0 + \cos^2\eta)^{\frac{1}{2}}} = \nu\frac{\partial^2 v}{\partial x_3^2},$$

$$\frac{\partial w}{\partial x_3} + \frac{u\cot\eta}{c(\sinh^2\xi_0 + \cos^2\eta)^{\frac{1}{2}}} + \frac{1}{c(\sinh^2\xi_0 + \cos^2\eta)^{\frac{1}{2}}}\frac{\partial u}{\partial \eta} = 0,$$

subject to

$$t < 0: \qquad u = v = w = 0,$$

$$t > 0: \qquad \begin{cases} u = w = 0, & v = c\Omega\cosh\xi_0\sin\eta, \quad \text{on} \quad x_3 = 0, \\ u, v \to 0 \quad \text{as} & x_3 \to \infty. \end{cases}$$

The radius at the equator of the oblate spheroid is $c\cosh\xi_0$ which we identify with a, the radius of the sphere for purpose or comparison.

Following the procedure adopted in the spherical case let

$$u = \cos\eta \cdot \tilde{u}(x_3, t) + \ldots,$$

$$v = \tilde{v}(x_3, t) + \ldots,$$

$$w = \tilde{w}(x_3, t) + \ldots,$$

and in the equations for $\tilde{u}, \tilde{v}, \tilde{w}$ so obtained set $\eta = \pi/2$ to obtain local equations valid in the neighbourhood of the equator. The change of variables

$$\tilde{u} = c\Omega\cosh\xi_0 \cdot u',$$

$$\tilde{v} = c\Omega\cosh\xi_0 \cdot v',$$

$$\tilde{w} = (\nu\Omega\coth\xi_0)^{\frac{1}{2}} w',$$

$$x_3 = (\nu\Omega^{-1}\tanh\xi_0)^{\frac{1}{2}} z,$$

$$t = \tanh\xi_0 \cdot T\Omega^{-1},$$

yields equations and boundary conditions for u', v', w' identical to (8) and (9) for the sphere. Thus the solution of the local problem for the oblate spheroid is like that for the sphere with a suitable scaling. Moreover, since $|\tanh\xi_0| \leqslant 1$ it follows that if the singularity in the sphere problem arises at time $T = T^*$, then for an oblate spheroid rotating with the same angular velocity Ω the breakdown in real time will be earlier by a factor $\tanh\xi_0$. In particular, if ξ_0 is very small corresponding to an almost circular disc, the breakdown occurs very soon after the impulsive start. This is in agreement with the intuitive impressions that one may reasonably form.

The analysis for the prolate spheroid follows the same general pattern. With the usual prolate spheroidal coordinates (ξ, η, ϕ) and the spheroidal surface given by $\xi = \xi_0$, it is found that the appropriate time scaling is $t = \coth\xi_0 \cdot T\Omega^{-1}$ corresponding to a slowing down of the development relative to that of the spherical case.

REFERENCES

[1] A. Davey, Boundary-layer flow at a saddle point of attachment, *J. Fluid Mech.* 4 (1961) 593-610.
[2] H. Blasius, Grenzschichten in Flüssigkeiten mit kleiner Reibung, *Z. Math. Phys.* 56 (1908) 1-37.
[3] I. Proudman & K. Johnson, Boundary-layer growth near a rear stagnation point, *J. Fluid Mech.* 12 (1962) 161-168.
[4] D. P. Telionis & D. Th. Tsahalis, Unsteady laminar separation over impulsively moved cylinders, *Acta Astronautica* 1 (1974) 1487-1505.
[5] F. T. Smith & P. W. Duck, Separation of jets or thermal boundary layers from a wall, *Quart. Jour. Mech. Appl. Math.* XXX (1977) 143-156.
[6] S. D. Nigam & R. S. I. Rangasami, Growth of boundary layer on a rotating sphere, *Z. angew. Math. Phys.* 4 (1953) 221-223.
[7] W. H. H. Banks, *The three-dimensional laminar boundary layer on a rotating sphere and other topics.* Ph. D. dissertation, University of Bristol (1963).
[8] W. H. H. Banks, The laminar boundary layer on a rotating sphere, *Acta Mechanica* 24 (1976) 273-287.
[9] R. J. Bodonyi & K. Stewartson, The unsteady laminar boundary layer on a disk in a counter-rotating fluid, *J. Fluid Mech.* 79 (1977) 669-688.
[10] H. Ockendon, An asymptotic solution for steady flow above an infinite rotating disc with suction, *Quart. Jour. Mech. Appl. Math.* XXV (1972) 291-301.